# Chapter 4

# An Empirical Analysis of State-of-the-Art Classifiers for Recognition of Hand Gestures using Existing Features

In image processing, feature describes the pattern of an image. Feature extraction and feature selection are two important steps in machine learning, pattern recognition and image processing. Feature extraction is the transformation of an initial set of features into a derived set of more informative and non-redundant features. On the other hand feature selection is the process of selecting subset of feature optimizing a certain criteria function. In this chapter, an analysis on recognition of SSHG using five state of the art classifiers viz., k-nearest neighbor (k-NN), naive Bayes, Bayesian network, decision tree and Support Vector Machine (SVM) is presented. In this analysis, different feature sets viz., Hu's invariant moments, Zernike moments, Legendre moments and 14 geometric features are used. It is observed that the feature set containing Legendre moments gives better performance than the other feature sets.

The rest of the chapter is organized as follows: Section 4.1 presents the related work in this domain. Section 4.2 provides the overview of features used in this chapter. Section 4.3 defines the theory of the state-of-the-art classifier. Experimental results are discussed in Section 4.4. Finally, Section 4.5 gives the observation of this chapter with the scope of future work.

## 4.1 Related Works

Historically, M.K. Hu is the pioneer in research on image analysis using statistical moments in the year 1961 [11]. He used geometric moment for automatic character recognition. Later, in 1962 this method was applied in the area of pattern recognition [2]. Then from 1971 onward, the moment invariant methods are used for ship identification [72], artifact identification [13], pattern matching [12]. The most popular work was done by Teague in 1980, who introduced the concept of orthogonal moment for the first time and provided the basic concept on Legendre and Zernike moment [77]. In 1981 [61], the geometric moment became extended to radial moments and provided a general framework for deriving radial and angular invariants. The complex moments was introduced in 1984 [1] and, in 2003 [83] another orthogonal moments Krawtchouk polynomial was introduced. This Krawtchouk moment was extended to a new radial Krawtchouk moment using polar representation of an image in 2007 [81]. Some of the work on recent moments are (i) Object identification using a neural network [33] and Zernike moments invariants. (ii) Fuzzy quaternion approach to object recognition using Zernike moments invariant 1990 [52]. (iii)Gesture recognition via pose classification [51]. Some more work in the area of pattern recognition using moment are found in [6, 69]. In this chapter, Hu's invariant moment, Zernike orthogonal moment, Legendre moment and geometric features are applied on Sattriya dance dataset. The description of shape representation using moment features are discussed in the following Table 4.1.

Table 4.1: Description of Shape Representation using Moment Features

| Moment Features | Symbol | Description |
|---|---|---|
| Zero-order | $M_{00}$ | Total intensity of an image and geometrical area for |
| First-order | $x_0 = M_{10}/M_{00}$, $y_0 = M_{01}/M_{00}$ | Centroid of the image |
| Second- order | $\mu_{20}, \mu_{02}, \mu_{11}$ | $\mu_{20}, \mu_{02}$ variance or distribution of horizontal and vertical projection,$\mu_{11}$gives covariance measure [48]. |
| Third - order | $\mu_{30}, \mu_{03}$ | Skewness of the image projection, i.e., degree of deviation [48] |
| Fourth - order | $\mu_{40}, \mu_{04}$ | Kurtosis of images i.e., measure the flatness and peakness of images [48]. |

## 4.2 Computation of Feature Sets

In this chapter, four feature sets were extracted from the SSHG image dataset. The four feature sets consist of Hu's seven invariant moments (FS1), Orthogonal Zernike moment up to tenth order (FS2) and Orthogonal Legendre moments up to tenth order (FS3) and 14 Geometric features (FS4). Each feature set is described briefly in the remaining part of this section.

### 4.2.1 Hu's Seven Invariant Moments (FS1)

Hu's invariant moments are based on second and third order central moments. The Hu's moment feature set is computed on three different images viz., gray image, binary image and extracted boundary image. Then, the extracted features set for different images are experimented on standard classifier such as k-nearest neighbor (k-NN), naive Bayes, Bayesian Network, decision tree and Support Vector Machine (SVM). The extraction of Hu's moment features from the image dataset is described briefly as follows: The geometric moment of order (p+q) of a two dimensional image f(x,y) of size $M \times M$ are defined as [11, 77]

$$m_{pq} = \sum_{x=1}^{M} \sum_{y=1}^{M} x^p y^q f(x, y) \tag{4.1}$$

p, q=$0, 1, 2, \ldots \infty$ where 'p+q' represent the order of the moment and f$(x, y)$ denotes the intensity of the pixel at location (x,y).
When the function $f(x, y)$ is translated by $f(x', y')$ then central moment can be written as:

$$\mu_{pq} = \sum_{x=1}^{M} \sum_{y=1}^{M} (x - x')^p (y - y')^q f(x, y) \tag{4.2}$$

Where, $f(x', y')$ represents the centroid of the image which can be defined as $x' = m_{10}/m_{00}$ and $y' = m_{01}/m_{00}$. The Hu's seven invariant moments viz.,$\phi_1, \phi_2, \ldots \phi 7$ are defined using central [48] moments as follows:

$$\phi_1 = \mu_{20} + \mu_{20} \tag{4.3}$$

$$\phi_2 = (\mu_{20} - \mu_{20})^2 + 4\mu_{11} \tag{4.4}$$

$$\phi_3 = (\mu_{30} - 3\mu_{12})^2 + 3(\mu_{21} - \mu_0 3)^2 \tag{4.5}$$

$$\phi_4 = (\mu_{30} + \mu_{12})^2 + (\mu_{21} + \mu_0 3)^2 \tag{4.6}$$

$$\phi_5 = (\mu_{30} - 3\mu_{12})(\mu_{30} + \mu_{12})[(\mu_{30} + \mu_{12})^2 - 3(\mu_{21} + \mu_{03})^2] \mid$$

$$+3(\mu_{21} - \mu_{03})(\mu_{21} + \mu_{03})[3(\mu_{30} + \mu_{12})^2 - (\mu_{21} + \mu_{03})^2] \quad (4.7)$$

$$\phi_6 = (\mu_{20} - \mu_{02})[(\mu_{30} + \mu_{12})^2 - (\mu_{21} + \mu_{03})^2] - 4\mu_{11}(\mu_{30} + \mu_{12})(\mu_{21} + \mu_{03}) \quad (4.8)$$

$$\phi_7 = (3\mu_{21} - \mu_{03})(\mu_{30} + \mu_{12})[(\mu_{30} + \mu_{12})^2 - 3(\mu_{21} + \mu_{03})^2]$$

$$-(\mu_{30} + 3\mu_{12})(\mu_{21} + \mu_{03})[3(\mu_{30} + \mu_{12})^2 - (\mu_{21} + \mu_{0}3)^2] \quad (4.9)$$

As an example, Hu's moment invariants of the binary image of the Alpadma hasta of SSHG are shown in Figure 4-1.

| Hu's moment Features set(hf1, hf2, …., hf7) | | | | | | | Images |
|---|---|---|---|---|---|---|---|
| 0.226307 | 0.002844 | 0.000857 | 0.000615 | 0.00001 | 0.000033 | -1E-06 | 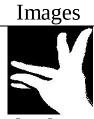 P1_alpadma_n_1 |
| 0.231371 | 0.002896 | 0.001408 | 0.000676 | 0.00001 | 0.000036 | -1E-06 |  P1_alpadma_n_8 |
| 0.231833 | 0.002599 | 0.001547 | 0.000651 | 0.00002 | 0.000033 | -1E-06 |  P1_alpadma_n_10 |

**Figure 4-1:** Example of Hu's Moment Invariants

### 4.2.2 Zernike Moment Feature Set (FS2)

Shape analysis using Zernike moment gained popularity among researchers in pattern recognition and image analysis for their invariance and orthogonal property. Zernike moment of order n is defined as

$$Z_(pq) = \frac{(n+1)}{\pi} \int_0^{2\pi} \int_0^{1} V^*_{pq(\rho,\theta) f(\rho,\theta)} \quad (4.10)$$

Here, p represents the non negative integer and q is an integer with constraint $(p - |q|)$ is even. Here $q < p$ and p and q denote the order of Zernike basis function.

The kernel of Zernike moments is the orthogonal Zernike polynomial, defined over the polar co-ordinate inside a unit circle. If $(\rho, \theta)$ is a polar co-ordinate. Mathematically, Zernike polynomial $V_{pq}(\rho, \theta)$ can be defined over unit disk as [48]

$$V_{pq}(\rho, \theta)) = R_{pq}(\rho)^{(jp\theta)} where \rho <= 1 \quad (4.11)$$

where $R_{pq}(\rho)$ is a real valued radial polynomial given by

$$R_{pq}(\rho) = \sum_{s=0}^{\frac{(p-|q|)}{2}} (-1)^s \frac{(p-s)!}{s!(\frac{(p+|q|)}{2}-s)!(\frac{(p-|q|)}{2}-s)!} \tag{4.12}$$

Zerinke moments rotation invariant, robust with respect to noise and minor variation and have no information redundancy. Example of Zernike moment features are shown in Figure 4-2.

| Zernike moments features set(zf_00, zf_11, zf_20, zf_22, zf_31, zf_33 ....., z_10,8 zf_10,10) | | | | | | | | Images |
|---|---|---|---|---|---|---|---|---|
| 0.172431 | 0.028302 | 0.173894 | 0.31329 | 0.13100 | 0.074291 | 0.113188 | 0.15827 | 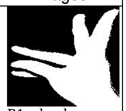 |
| 0.055803 | 0.137155 | 0.078724 | 0.04778 | 0.075533 | 0.0603 | 0.08723 | 0.055142 | |
| 0.051437 | 0.059085 | 0.050106 | 0.026837 | 0.010276 | 0.024235 | 0.088369 | 0.088417 | |
| 0.116435 | 0.053791 | 0.021734 | 0.022582 | 0.04972 | 0.04494 | 0.031011 | 0.034657 | |
| 0.018418 | 0.039866 | 0.1106596 | 0.021857 | | | | | P1_alpadma_n_ 1 |
| 0.183429 | 0.029496 | 0.173753 | 0.281164 | 0.129841 | 0.0376 | 0.109026 | 0.141683 |  |
| 0.063923 | 0.147185 | 0.018467 | 0.014684 | 0.074058 | 0.06774 | 0.084874 | 0.063923 | |
| 0.062294 | 0.079642 | 0.039269 | 0.085826 | 0.051286 | 0.036128 | 0.012923 | 0.062103 | |
| 0.100207 | 0.017034 | 0.028398 | 0.061205 | 0.110265 | 0.070097 | 0.04184 | 0.067717 | |
| 0.018404 | 0.054212 | 0.0944695 | 0.106535 | | | | | P1_alpadma_n_ 10 |

**Figure 4-2:** Example of Zernke Moments of Order 0 to 10

### 4.2.3 Legendre Moments Feature Set (FS3)

This Legendre moment feature set is based on Legendre polynomial which was introduced by M. R. Teague [77]. The Legendre moments of order p+q is defined as follows [48, 69, 77]:

$$L_{pq} = \frac{(2p+1)(2q+1)}{4} \int_{-1}^{1}\int_{-1}^{1} P_p(x)P_q(y)f(x,y)dxdy \tag{4.13}$$

where the function $P_p(x)$ denotes the Legendre polynomial of order p. If $f(i,j)$ represents the pixel value at the $(i,j)$th pixel of a $N \times N$ image, then the Legendre moments can be approximated by the following equation:

$$L_{pq} = \frac{(2p+1)(2q+1)}{(N-1)^2} \sum_{i=1}^{N}\sum_{j=1}^{N} P_p(x_i)P_q(y_j)f(i,j) \tag{4.14}$$

Here, $(x_i, y_j)$ represents the normalized pixel in the range [-1, 1], given by $x_i = (2i/N) - 1, y_j = (2j/N) - 1$.
The Legendre polynomial $P_n(x)$ of order $n$ is defined as:

$$P_n(x) = \sum_{k=0}^{n} (-1)^{(n-k)/2} \frac{1}{2^n} \frac{(n+k)!x^k}{(\frac{n-k}{2})!(\frac{n+k}{2})!k!}, \tag{4.15}$$

Here, $|x| \leq 1$ and (n-k) is even.
The recursive relation for Legendre polynomials can be written in simplified form as [48]

$$P_n(x) = \frac{(2n-1)xP_{n-1}(x) - (n-1)P_{n-2}(x)}{n} \tag{4.16}$$

Here $P_0(x) = 1; P_1(x) = x; n > 1$
Example of the Legendre moments of order 0 to 10 of two images are shown in Figure 4-3.

| Legendre-Moment Features Sets(lf_1, lf_2,......lf_66) | | | | | | | | Images |
|---|---|---|---|---|---|---|---|---|
| 0.55715 | -0.24269 | -0.34309 | 0.260251 | -0.16117 | 0.216378 | 0.135369 | -0.29001 |  |
| 0.221406 | 0.379455 | -0.04498 | -0.27579 | -0.45886 | 0.155347 | 0.265961 | -0.17061 | |
| 0.332198 | -0.38218 | -0.18008 | -0.07141 | -0.06071 | 0.089528 | 0.14064 | -0.08145 | |
| 0.279011 | -0.3629 | -0.08038 | 0.005706 | 0.13 | -0.06903 | 0.080343 | -0.32578 | |
| 0.341077 | 0.032694 | 0.021267 | 0.025678 | -0.02177 | -0.11558 | 0.124088 | -0.33445 | |
| 0.255655 | -0.1425 | 0.233067 | -0.13065 | -0.02946 | -0.06636 | 0.097534 | -0.11631 | |
| 0.275682 | -0.00325 | -0.18003 | -0.40015 | 0.418341 | -0.17782 | -0.1287 | -0.02326 | P1_alpadma_n_1 |
| 0.000716 | 0.201391 | 0.109543 | 0.003137 | 0.193929 | -0.55 | 0.073072 | 0.233228 | |
| 0.097782 | -0.19252 | | | | | | | |
| 0.539775 | -0.17977 | -0.22511 | 0.265304 | -0.11936 | 0.442221 | 0.015752 | -0.248506399 |  |
| 0.381235 | 0.332068 | -0.15343 | -0.16915 | -0.31591 | 0.375689 | -0.01185 | -0.034064876 | |
| 0.233635 | -0.41317 | -0.01191 | 0.033154 | -0.05483 | 0.150877 | -0.07764 | 0.081768892 | |
| 0.158677 | -0.27804 | -0.10862 | 0.150451 | -0.00196 | -0.11221 | -0.03716 | -0.122251659 | |
| 0.479702 | 0.038038 | -0.35893 | -0.0092 | -0.04255 | -0.06843 | -0.14848 | -0.2571283 | |
| 0.273294 | -0.02722 | 0.511985 | -0.36658 | -0.21302 | -0.03597 | 0.042881 | -0.047484167 | |
| 0.216788 | -0.27229 | -0.08266 | 0.232763 | 0.343635 | 0.050364 | -0.16838 | -0.0054431 | |
| 0.124197 | 0.138278 | -0.06389 | 0.14192 | 0.232944 | -0.6361 | 0.50301 | -0.178423105 | P1_alpadma_n_10 |
| 0.08776 | -0.1827 | | | | | | | |

**Figure 4-3:** Example of Legendre Moments of Order 0 to 10

### 4.2.4 Geometric Feature Set (FS4)

Geometric features are those features which describe the shape of the images. Initially, 14 types of geometric features Viz., area, centroid, eccentricity, bounding box, aspect ratio, convex hull, equiv diameter, Euler number, major axis length, minor axis length, orientation, perimeter, max intensity, min intensity are extracted. To improve the recognition performance, Attribute Ranking (Information Gain Ranking Filter) feature selection method is used to choose the suitable features. Rank of the attributes given by this features selection method are as follows:

- Centroid(0.35)
- Eccentricity(0.269)
- Orientation(0.256)
- Major Axis Length(0.215)
- Minor Axis Length(0.210)
- Aspect Ratio(0.195)

- Perimeter(0.194)
- Area(0.17)
- BoundingBox(0.0)
- Orientation(0.0)
- EulerNumber(0.0)
- EquivDiameter(0.0)
- Perimeter(0.0)
- MeanIntensity(0.0)
- MinIntensity(0.0)
- MaxIntensity(0.0)

On the basis of this ranking, the 8 features with non-zero ranks are selected and used throughout this experiment. This 8 features of feature set FS4 are briefly described as follows [58]:

- Centroid: Centroid of the image can be defined as center of mass of the object. For a 2D image $f(x, y)$ (x=1,2,, M)and (y=1,2, . . . , M) of size $M \times M$, the centroid $(\bar{x}, \bar{y})$ is given by

$$\bar{x} = \frac{\sum\limits_{x}\sum\limits_{y} x.f(x,y)}{\sum\limits_{x=1}^{M}\sum\limits_{y=1}^{M} f(x,y)}, \bar{y} = \frac{\sum\limits_{x}\sum\limits_{y} y.f(x,y)}{\sum\limits_{x=1}^{M}\sum\limits_{y=1}^{M} f(x,y)} \tag{4.17}$$

- Eccentricity: The eccentricity of an image can be defined as the ratio of the distance between the foci of the object to its major axis length.
- Orientation: The orientation represents the angle (in degrees) between the x-axis and the major axis of the object.
- Bounding Box: The bounding box is the smallest rectangle that contain the object. For an image, the diagonal pixel points represent the bounding box.
- Major Axis Length: The major axis length is the length of the longest diameter of an object.
- Minor Axis Length: The minor axis length is the length of the shortest diameter of the object.
- Aspect Ratio: The aspect ratio can be measured by the ratio of the width to the height of the object.

- Perimeters: A pixel in a binary image is a perimeters pixel if it is non-zero and it is connected to at least one zero-valued pixel. The default connectivity is 4 for two dimensional images. In this experiment the attribute is taken to be the length (number of pixels) of the perimeter.

Example of the geometric feature set (comprises of 14 features) is shown in Figure 4-4

| Geometric features set(G_1, G_2,......G_14) | Images |
|---|---|
| 860.56521 93.51949 49.04347 11.53709 9.750137 0.419399 -2.53190<br>-9.652173 8.675686 88.06304 18.22882 5.869565 22.52173 -6.17061 | <br>P1_alpadma_n_1 |
| 855.55221 92.94951 50.03447 11.63709 9.82337 0.428399 -2.43190<br>-9.501273 8.775686 88.16314 18.21222 5.903565 21.52233 -6.27161 | <br>P1_alpadma_n_10 |

**Figure 4-4:** Example of Geometric Feature Set

# 4.3 Classifiers

Classification means mapping the images into predefined classes i.e., it is the function from the feature space to the output class. The classifiers used in this chapter are described briefly in this section.

## 4.3.1 k-Nearest Neighbor

k-Nearest Neighbor classifieris (k-NN) [18] is a supervised classifier. It uses distance based similarity measure to classify an unknown object to one of the known classes. Given an unknown object or pattern the k-NN classifier searches for the k training pattern which are closest to the given unknown pattern or objects. These k training pattern are the k-nearest neighbor of the unknown pattern. The unknown pattern is assign the most common class among its k-nearest neighbors. For two objects X and S with feature vectors $(x_1, x_2, \ldots..., x_N)_T$ and $(s_1, s_2, \ldots..., s_N)_T$, some of the distance are defined in terms of mathematical formula as follows:

$$Euclidean = \sqrt{\sum_{i=0}^{N}(xi - si)^2} \tag{4.18}$$

$$Manhattan = \sum_{i=0}^{N} \mid xi - si \mid^2 \tag{4.19}$$

$$Minkowski = (\sum_{i=0}^{N} (\mid xi - si \mid)^q)^{\frac{1}{q}} \tag{4.20}$$

$$Hamming(D) = \sum_{i=0}^{N} \mid xi - si \mid^2 \tag{4.21}$$

**k-value determination**

If k=1, then the nearest neighbor case is simply assign to that class. Generally, the value of k has to be selected by the user and it can be randomly increased for large dataset. The k-value which gives minimum error rate is selected. If the value of k is large, then it helps to reduce the noise effect in classification. Although k-NN algorithm is very simple but problem is when we apply the distance directly on training set with variable of different measure scale. So, we need to standardize the distance with the given formula.

$$Newvalue(Xz) = \frac{Originalvalue - Minvalue}{Maxvalue - Minvalue}. \tag{4.22}$$

In our experiment, we use k=5 for feature set which gives low error rate on SSHG dataset. We use Euclidean distance as it gives good results compared to other distancce. Limitation of k-NN algorithm is that it is time consuming for large training data.

### 4.3.2 Naive Bayes

Naive Bayes [18] classifier is one of the Bayesian classifier which can predict class membership using different probability convention. The Bayesian classifier model is very popular model because of its simplicity, also no complicated iterative parameter estimation required. This classifier is suitable for very large dimension of data set. The model of this classifier can be done in two ways: with class posterior probability known as discriminative model and the alternate way is to learn the class conditional density. The Naive Bayes classifier work based on a training set of objects and their associated class level. We consider $y_1, y_2, y_3, \dots y_m$ are m classes and X is the object of the classifier which belongs to the class having highest probability. Then, the Naive Bayes classifier predicts that the object X belongs to the class $y_i$ if

$$P(y_i/X) > P(y_j/X) \tag{4.23}$$

for 1 $\leq$j$\leq$m and j$\neq$i
The SSHG dataset is tested on Naive Bayes classifier and results are discussed in next section.

#### 4.3.2.1 Bayesian Network

Bayesian Networks(BN) [17] is an expert system, captures all the existing knowledge. It is the succeed way to represent any distribution. This classifier mainly deals with the uncertainty of random variable. It is graphically shown by Directed Acyclic Graph(DAG) where each node represent the random variable and arc represent the dependency between the nodes. Representation of Bayesian Networks is shown in Figure 4-5 The

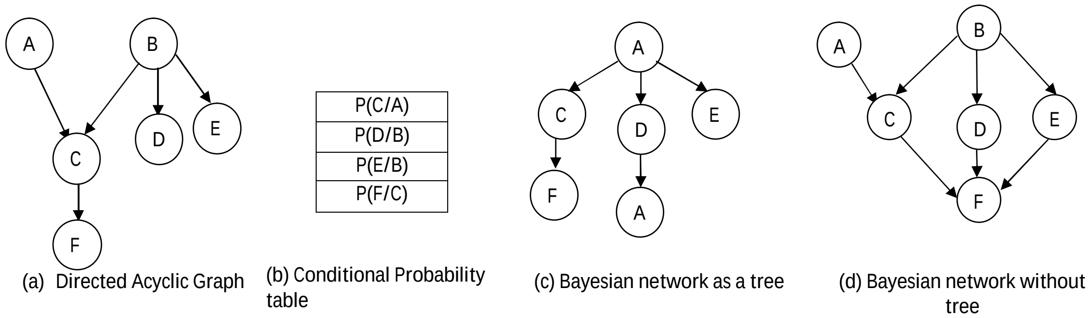


**Figure 4-5:** Representation of Bayesian Network

directed graph $X \rightarrow Y$ provides information that X has direct control on Y, and X is said to be parent of Y.
Each value of probability density function is computed as

P[x$_1, x_2 \ldots x_n] = P[x_1/x_2 \ldots x_n]$
$= P[x_1/x_2 \ldots, x_n].P[x_2/x_3][x_{n-1}/x_n]P[x_n]$
$= P[x_i/x_{i+1}, \ldots, x_n]$
(4.24)Convention of Bayesian Network:
$P(X) = \pi(P(X_i)/P_a(X_i))$ where $X = X_1, X_2, \ldots, X_n$ are nodes. $P(X_i)$ is the joint probability of nodes X $Pa(X_i)$ are parent node of $X_i$

### 4.3.3 Decision Tree

Decision Tree [56] is a tree which correctly classify the objects in the training set. Each of the leaf node represent the class, all internal nodes denote attribute-based test and branches are used for each possible outcome. The path from root node to leaf node denotes classification convention. To classify any objects, it is necessary to start visiting the tree from root node, evaluate the test at each node and take the branch which is appropriate for the outcome of the test. This procedure continue until find the leaf node and the object is classified base on the class label of the leaf node.

### 4.3.4 Support Vector Machine (SVM)

It is the most common supervised learning algorithm. Generally, SVM is a binary classifier (separate two classes) however multiple SVMs could be used for multi-class classification. SVM uses hyperplane as decision boundary which separates the two classes by maximizing the distance or gap between two classes. The object which are closed to the decision boundary on its either side are called support vector. Optimal decision boundary depends only those support vector.

The multiclass SVMs are generated by combining multiple two class SVM. There are two popular techniques of obtaining multiclass SVM. (i) one vs one and (ii) one vs rest [21]. The SVM classifier works as follows: Considering, D as the given dataset as $(x_1, y_1)$, $(x_2, y_2)$, $\ldots (x_D, y_D)$ where $x_i$ is the training sample and $y_i$ represent the corresponding class label whose value varies between -1 and 1. The training tuple X can be written as $(x_1, x_2)$ where $x_1, x_2$ are the attributes. The SVM gives the solution for the below mentioned optimization problem. $\min_{w,h,\epsilon} \frac{1}{2} W^T W + C \sum_{i=1}^{n} \epsilon_i$

subject to $\mathrm{y}_i(w^T \phi(x_i) + b) \geq 1 - \epsilon, \epsilon \geq 0$ In this classification, the vector $x_i$ is mapped to the higher dimension by changing the value of $\phi$. The kernel function of SVM is

$\mathrm{K}(\mathrm{x}_i, x_j) = \phi(x_i)^T \phi(x_j)$ and $C > 0$ is known as penalty parameter. There are three type of kernel function used for SVM classifier:

1. Linear: $K(x_i, x_i) = {x_i}^T x_j$.
2. Polynomial:$K(x_i, x_i) = (\gamma {x_i}^T x_j + r)^d, \gamma > 0$
3. Radial Basis Function(RBF): $K(x_i, x_j) = exp(-\gamma \mid\mid x_i - x_j \mid\mid^2), \gamma > 0$

## 4.4 Experimental Results

The experiments have been carried out on a PC with intel i5 processor containing 4 GB main memory and 500 GB hard disk running 64 bit windows10 operating system. MATLAB 2015 is used for the experiments.

### 4.4.1 Dataset Description

The experiments are conducted using Sattriya Dance single-hand gestures (SSGH) dataset developed by us as part of this research work. The dataset has both original images and additional instances generated by adding artificial noise. The description about creation of the SSHG dataset are discussed

Table 4.2: Dataset Description

| Dataset | Instances | Feature set | Attributes |
|---|---|---|---|
| SSHG (without noise) | 1450 | FS1 | 7 |
| | | FS2 | 36 |
| | | FS3 | 66 |
| | | FS4 | 14 |
| SSHG (with noise) | 44,950 | FS1 | 7 |
| | | FS2 | 36 |
| | | FS3 | 66 |
| | | FS4 | 14 |

in the previous Chapter 3

### 4.4.2 Performance Analysis on SSHG Dataset Without Noise

Four types of feature-dataset FS1, FS2, FS3 and FS4 are computed from SSHG dataset. These features set are experimented on different state-of-the-art classifiers such as k-nearest-neighbor (k-NN), naive Bayes , Bayesian network, decision tree and Support Vector Machine (SVM). For each classifier, 70% (1015) instances are used for training and remaining 30% (435) instances are used to validate the results. The experimental outcome on SSHG dataset with noise and without noise with five well known classifiers are discussed as follows:

#### 4.4.2.1 Performance Analysis on Feature set FS1

The feature set FS1 consists of seven invariant features. The feature set is experimented on three type of images viz., gray-image, binary-image and boundary-image for behavior analysis of images. The recognition accuracy achieved for FS1 with the four state of art classifiers excluding SVM are shown in Table 4.3.

Table 4.3: Recognition Results on FS1

| Dataset | Classifier | Total instances | Correctly classified | Average recognition rate |
|---|---|---|---|---|
| Gray-image | k-NN(n=5) | 435 | 302 | 69.43 |
| | Bayesian Network | 435 | 274 | 62.99 |
| | Nave Bayes | 435 | 221 | 50.80 |
| | Decision Tree | 435 | 318 | 73.10 |
| Binary-image | k-NN(n=4) | 435 | 336 | 77.24 |
| | Bayesian Network | 435 | 270 | 62.07 |
| | Nave Bayes | 435 | 385 | 88.51 |
| | Decision Tree | 435 | 416 | 93.63 |
| Boundary-Extracted image | k-NN (n=5) | 435 | 311 | 71.49 |
| | Bayesian Network | 435 | 316 | 72.64 |
| | Nave Bayes | 435 | 308 | 70.80 |
| | Decesion Tree | 435 | 350 | 80.45 |

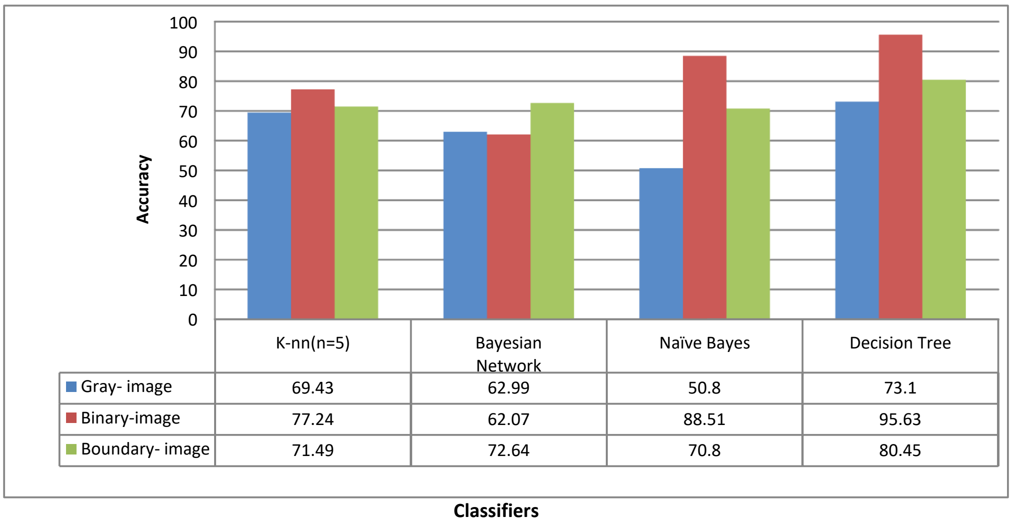


**Figure 4-6:** Comparative Performance on SSHG Dataset using FS1

The comparative performance of the classifiers using FS1 can also be observed from the graph given in Figure 4-6. From the above graph, it can be observed that binary image dataset provides good results for most of the classifier. Therefore, the remaining experiments carried out on binary image dataset.

Table 4.4: Recognition Accuracy of Four Feature Set with State of Art Classifier

| Feature sets | Classifiers | Total instances | Correctly classified | Classification Accuracy |
|---|---|---|---|---|
| Hu's moment | SVM Linear Kernel (C=1, E=1) | 435 | 296 | 68.05 |
| | SVM Polynomial (C=3, E=4) | 435 | 288 | 65.20 |
| | SVM RBF (C=9, $\gamma$=.033) | 435 | 309 | 71.03 |
| Zernike moment | k-NN(n=5) | 435 | 304 | 69.65 |
| | Bayesian Network | 435 | 153 | 34.94 |
| | Nave Bayes | 435 | 122 | 28.04 |
| | Decision Tree | 435 | 309 | 71.03 |
| | SVM-Linear Kernel(c=1, E=1) | 435 | 303 | 69.65 |
| | SVM-polynomial | 435 | 296 | 68.04 |
| | SVM-RBF(c=9, gamma=.033) | 435 | 314 | 72.18 |
| Legendre moment | k-NN(n=5) | 435 | 315 | 72.41 |
| | Bayesian Network | 435 | 384 | 88.27 |
| | Nave Bayes | 435 | 393 | 90.34 |
| | Decision Tree | 435 | 418 | 96.09 |
| | SVM-Linear Kernel(c=1, E=1) | 435 | 411 | 94.48 |
| | SVM-polynomial | 435 | 405 | 93.10 |
| | SVM-RBF(c=9, gamma=.033) | 435 | 395 | 90.80 |
| Geometric | k-NN(n=5) | 435 | 175 | 40.22 |
| | Bayesian Network | 435 | 55 | 12.64 |
| | Nave Bayes | 435 | 122 | 28.04 |
| | Decision Tree | 435 | 296 | 68.04 |
| | SVM-Linear Kernel(c=1, E=1) | 435 | 270 | 62.06 |
| | SVM-polynomial | 435 | 182 | 42.06 |
| | SVM-RBF(c=9, gamma=.033) | 435 | 285 | 65.51 |

The performance of SVM classifier using FS1 on binary image dataset with linear kernel, polynomial kernel and the radial basis kernel (RBF) is shown in Table 4.4. It can be observed from this experiment that RBF kernel gives better results compared to other kernels.

#### 4.4.2.2 Classification result on FS2

The feature set FS2 i.e., Zrenike moment features upto tenth order were extracted from the SSHG-binary image dataset . The recognition accuracy for this feature set is shown in Table 4.4. Here also, the SVM with RBF kernel provides good result compared to other classifiers with accuracy 72.18%. The different kernel parameter C and E are set for polynomial kernel, which were obtained by varying the value within a range. For this kernel, C denote the complexity parameter and E is the exponent. Also the parameter C and $\gamma$ for RBF kernel were determind by Grid Search algorithm [24]. In this classifier, the parameter C control the cost of miss classification and $\gamma$ represent the Gaussian kernel to handle nonlinear classification. It is graphically represented by a peak. A small $\gamma$ gives a sharp peak in the higher dimension and large $\gamma$ gives softer peak.

#### 4.4.2.3 Classification result on FS3

The feature set FS3 comprises 66 features which were extracted using Legendre moment upto tenth order. The recognition accuracy for feature set FS4 has been shown in Table 4.4. From the table it can be concluded that Decesion tree classifier gives good result with 96.09% accuracy.

#### 4.4.2.4 Performance Analysis on Feature set FS4

The feature set FS4 (geometric features) includes 8 statistical features viz., centroid, eccentricity, orientation, major axis length, minor axis length, aspect ratio, perimeter are used throughout this experiment. The overall recognition accuracy for geometric feature set is poor as compared to other feature sets. The highest recognition accuracy rate is given by decision tree classifier which is 68.04% as shown in Table 4.4.

#### 4.4.2.5 Comparative Performance Analysis

The overall recognition accuracy for all the feature sets FS1, FS2, FS3, FS4 are presented in the above tables. The comparative performance on SSHG dataset is shown graphically in figure 4-7. From the graph it can be observed that the feature set FS3 (Legendre moments) provides the highest recognition accuracy for each classifier.

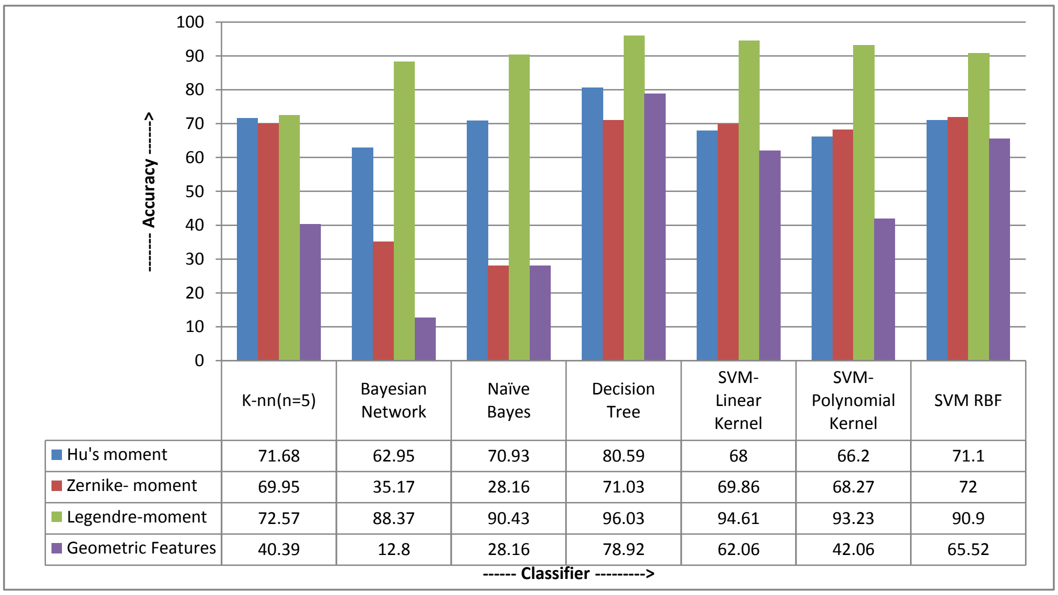


| | K-nn(n=5) | Bayesian Network | Naïve Bayes | Decision Tree | SVM-Linear Kernel | SVM-Polynomial Kernel | SVM RBF |
|---|---|---|---|---|---|---|---|
| Hu's moment | 71.68 | 62.95 | 70.93 | 80.59 | 68 | 66.2 | 71.1 |
| Zernike- moment | 69.95 | 35.17 | 28.16 | 71.03 | 69.86 | 68.27 | 72 |
| Legendre-moment | 72.57 | 88.37 | 90.43 | 96.03 | 94.61 | 93.23 | 90.9 |
| Geometric Features | 40.39 | 12.8 | 28.16 | 78.92 | 62.06 | 42.06 | 65.52 |

**Figure 4-7:** Comparative Performance of the Four Feature Sets on SSHG Dataset Without Noise

### 4.4.3 Performance Analysis on SSHG Dataset With Noise

Total number of instances of SSHG (with noise) dataset is 44,950. Experiments similar to the ones presented in section 4.4.2 have been conducted on this dataset to see the robustness of the features. For these experiments, 31,465 instances are used for training and 13,485 instances are used for testing. The recognition accuracies for the four feature sets and the five classifier on SSHG dataset with noise have been shown in Table 5.2. The comparative performance can be observed from the graph presented in Figure 4-8.

It can be observed from the graph that the classifier give similar performances on the both SSHG dataset with noise and without noise. Also it can be observed that the recognition accuracies increases with more number of instances as shown by the higher recognition accuracies on the dataset with noise.

## 4.5 Discussion

In this chapter, an empirical analysis of state of the art classifiers for recognition of single-hand gestures (Asamyukta hasta) of Sattriya dance has been done. This experiments were done on both SSHG with noise and with-

Table 4.5: Recognition Accuracy on SSHG Dataset on Noise

| Feature set | Classifier | Total instances | Correctly classified instance | Accuracy (%) |
|---|---|---|---|---|
| Hu's Moment | k-NN(n=5) | 13,485 | 10,086 | 74.79 |
| | Bayesian Network | 13,485 | 8840 | 65.55 |
| | Nave Bayes | 13,485 | 9740 | 72.33 |
| | Decision Tree | 13,485 | 10206 | 75.68 |
| | SVM-Linear Kernel(c=1, E=1) | 13,485 | 8813 | 65.35 |
| | SVM-polynomial | 13,485 | 8522 | 63.19 |
| | SVM-RBF(c=9, gamma=.033) | 13,485 | 10,925 | 81.01 |
| Zernike Moment | k-NN(n=5) | 13,485 | 9567 | 70.94 |
| | Bayesian Network | 13,485 | 8274 | 61.35 |
| | Nave Bayes | 13,485 | 7554 | 56.01 |
| | Decision Tree | 13,485 | 9210 | 68.30 |
| | SVM-Linear Kernel(c=1, E=1) | 13,485 | 8894 | 65.95 |
| | SVM-polynomial | 13,485 | 9342 | 69.28 |
| | SVM-RBF(c=9, gamma=.033) | 13,485 | 10113 | 75.00 |
| Legendre Moment | k-NN(n=5) | 13,485 | 10,012 | 74.25 |
| | Bayesian Network | 13,485 | 11,916 | 88.36 |
| | Nave Bayes | 13,485 | 10,576 | 78.43 |
| | Decision Tree | 13,485 | 11,601 | 86.03 |
| | SVM-Linear Kernel(c=1, E=1) | 13,485 | 12,464 | 92.43 |
| | SVM-polynomial | 13,485 | 11,223 | 83.23 |
| | SVM-RBF(c=9, gamma=.033) | 13,485 | 12,419 | 92.09 |
| Geometric | k-NN(n=5) | 13,485 | 6130 | 45.46 |
| | Bayesian Network | 13,485 | 5144 | 38.15 |
| | Nave Bayes | 13,485 | 4067 | 30.16 |
| | Decision Tree | 13,485 | 9196 | 68.09 |
| | SVM-Linear Kernel(c=1, E=1) | 13,485 | 8097 | 60.04 |
| | SVM-polynomial | 13,485 | 6076 | 45.06 |
| | SVM-RBF(c=9, gamma=.033) | 13,485 | 9982 | 74.02 |

out noise. Four feature sets Hu's seven invariant moment (FS1), Zernike moments (FS2), Legendre moments (FS3) and geometric feature (FS4) for

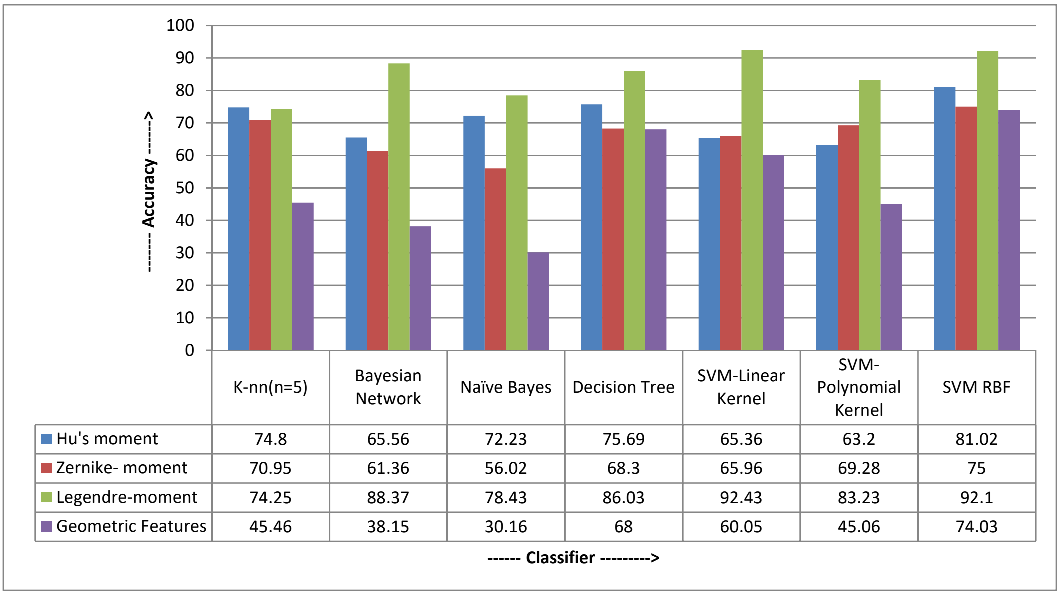


| | K-nn(n=5) | Bayesian Network | Naïve Bayes | Decision Tree | SVM-Linear Kernel | SVM-Polynomial Kernel | SVM RBF |
|---|---|---|---|---|---|---|---|
| Hu's moment | 74.8 | 65.56 | 72.23 | 75.69 | 65.36 | 63.2 | 81.02 |
| Zernike- moment | 70.95 | 61.36 | 56.02 | 68.3 | 65.96 | 69.28 | 75 |
| Legendre-moment | 74.25 | 88.37 | 78.43 | 86.03 | 92.43 | 83.23 | 92.1 |
| Geometric Features | 45.46 | 38.15 | 30.16 | 68 | 60.05 | 45.06 | 74.03 |

**Figure 4-8:** Comparative Performance of the Four Feature Sets on SSHG With Noise

performance analysis and five classifiers namely k-nearest neighbor, Bayesian network, naive Bayes, decision tree and SVM with different kernels are used. From the analysis, it can be observed that Legendre moments (FS4) show better performance compared to other feature sets. It is also observed that the recognition accuracy of geometric feature set (FS4) is the lowest. From the above discussion it can be concluded that for recognition of single-hand gestures of Sattriya dance, the features considered in this analysis are not suitable with the existing classifiers. Therefore, it is necessary to explore more suitable feature and also a better classifier for the purpose.